LWT - Food Science and Technology 163 (2022) 113588

Contents lists available at ScienceDirect

LWT

journal homepage: www.elsevier.com/locate/lwt

Nanoencapsulation of saffron *(Crocus sativus* L.*)* extract in zein nanofibers and their application for the preservation of sea bass fillets

Zahra Najafi [a,*], Turgay Cetinkaya [a,b], Fatih Bildik [a], Filiz Altay [a], Neşe Şahin Yeşilçubuk [a]

[a] Department of Food Engineering, Faculty of Chemical and Metallurgical Engineering, Istanbul Technical University, 34467, Maslak, Istanbul, Turkey
[b] Department of Food Processing, Armutlu Vocational School, Yalova University, 77500, Yalova, Turkey

ARTICLE INFO

Keywords:
Saffron extract
Electrospinning
Encapsulation
Preservation
Sea bass

ABSTRACT

In this study, saffron extract (SE) was encapsulated in zein nanofibers (ZNs) via electrospinning and then ZNs loaded with SE (ZNLSE) were applied as a nanocoating material. The effects of different zein concentrations (15%, 25%, and 30% w/v), SE concentrations (5% and 10% w/w) and the applied voltages on the morphology of ZNs were studied. The thermal stability of ZNs decreased with the addition of SE as determined by DSC. The molecular interaction between SE and zein was confirmed by ATR-FTIR. The encapsulation efficiency of crocins and picrocrocin, in ZNLSE (10%), were 64% and 47%, respectively assessed by HPLC. The antioxidant activity of ZNLSE (56.3%) was higher than that of the ZNs as assessed by ABTS method. Chemical deterioration in the control and coated fish fillets was monitored in terms of total volatile basic nitrogen (TVBN), thiobarbituric acid reactive substances (TBARS), peroxide value (PV), free fatty acid (FFA) and pH. The TVBN values of the treated samples were 30% lower than those of the control group on 8th day of cold storage. The results of this study indicated that ZNLSE has a significant potential as a coating material for prolonging the shelf lives of solid foods such as fish fillets.

1. Introduction

Saffron is attracting consumers' attention because it contains valuable bioactive compounds that exert imortant health-promoting effects. Crocins, picrocrocin, and safranal are the three main bioactive compounds identified in saffron stigmas. Special therapeutic benefits have been attributed to these compounds including antitumor activities, neuroprotective effects, antidepressant effects and enhancement of memory (Lambrianidou et al., 2021).

Crocins, the main components of saffron, are water-soluble carotenoids responsible for the desirable color of saffron and they consist of a group of crocetin glycosides (mono- and di-glycosyl esters of a dicarboxylic acid named crocertin). Picrocrocin, the second main component of saffron, is a monoterpene glycoside responsible for the its bitter taste. Safranal, the main volatile oil, is the product of the thermal or enzymatic degradation of picrocrocin and it contributes to the unique aroma of saffron (Ahmadian-Kouchaksaraie & Niazmand, 2017; Sarfarazi et al., 2019).

Crocin like other carotenoids is highly sensitive to degradation during food processing and storage due to consisting unsaturated ditrepene groups. The stability of crocin is affected by environmental factors including elevated temperature, light, oxygen, low pH, and the presence of metallic ions (Saroglu et al., 2021).

Nanoencapsulation techniques including nanoparticles, nanoemulsion and nanocapsules have been employed to avoid the degradation of bioactive compounds of saffron under undesirable conditions until their delivery to the physiological targets (Mirhadi et al., 2020). In this context, electrospinning and electrospraying technologies have gained increased interest for the encapsulation of bioactive ingredients and food packaging. They are simple, versatile, and non-thermal and thereby more appropriate for the encapsulation of heat-sensitive compounds (Ansarifar & Moradinezhad, 2022; Cetinkaya et al., 2021).

In the present study, zein protein, which has high hydrophobicity and good electrospinnability, was used as a carrier polymer. It has been reported in previous studies that zein film has good barrier, mechanical, and thermal resistance properties, making it a desirable packaging material (Li et al., 2009; Wang et al., 2017).

It has been reported that saffron exhibits good antioxidant activity (AA) in biological systems (Okmen et al., 2016; Parray et al., 2015). However, the antioxidant and antibacterial activities of saffron extract (SE) in food products have received limited attention (Armellini et al., 2018; Bhat et al., 2021; Najafi et al., 2022). For instance, Aboutorab

* Corresponding author.
E-mail address: najafi@itu.edu.tr (Z. Najafi).

https://doi.org/10.1016/j.lwt.2022.113588
Received 22 September 2021; Received in revised form 2 May 2022; Accepted 20 May 2022
Available online 24 May 2022

et al. (2021) reported that delayed oxidation in shrimp and showed antibacterial activity. In this sense, the use of SE-loaded nanofibers for the coating of sea bass fillets is proposed in the present study as a novel technique to inhibit biochemical deterioration in fish meat.

This study was designed with three main objectives. The first was to encapsulate saffron by electrospinning and study the effects of zein concentration, SE concentration, and applied voltage on the morphology of the fibers. The second was to characterize encapsulated samples in terms of DSC and FTIR measurements including encapsulation efficiency. The third was to evaluate the AA of ZNs loaded with SE (ZNLSE) by ABTS assay and use ZNLSE as a coating layer on sea bass fillets to utilize its effectiveness in delaying chemical deterioration.

2. Materials and methods

2.1. Materials

Zein was purchased from Sigma-Aldrich (Germany). Dried stigmas of saffron were purchased from Jamshidi Marandi producer (Khorasan-e-razavi, Iran), during the season of 2020. Sea bass (*Dicentrarchus labrax*) samples were purchased from Metro Gross Market (Istanbul, Turkey). Crocin-4 with purity of % 98 was purchased from Biopurify Phytochemicals Ltd (Sichuan, China). Other solvents and reagents were obtained from Merck (Germany).

2.2. Preparation and identification of SE compounds by HPLC and LC-MS

Preparation method freeze-dried SE described in detail in our previous study (Najafi et al., 2021). The SE bioactive components were determined using a HPLC system (Shimadzu, Japan) which was equipped with a quaternary pump and a UV–Vis photodiode array detector (PDA). The Alltima column (C18 zorbax, 250 mm × 4.6 mm, 5 μm) was used. The elution solvents were as follows: 0.1% TFA in water (solvent A) and Methanol (solvent B). The elution was performed via gradient method: 50% B for 5 min, linearly increase to 100% in 30 min and kept at 100% for 5 min and then decreased into 50% for 1 min and kept for 10 min.

Trans-crocin-4 observed as the main peak in the HPLC chromatogram of SE at 440 nm. This compound was identified by comparing its retention time with its standard. For identification of other SE components, the sample was analyzed by a LC-MS system (Thermo Fisher Scientific, San Jose, USA). The fragmentation patterns, molecular weight and quantity of main bioactive molecules of SE detected by LC-MS, were completely reported in our previous study (Najafi et al., 2021).

The equations used for quantification of saffron compounds were as follows: for crocin-4 and other crocins:Y = 156331X, R2 = 0.999, for picrocrocin was: Y = 1952830X - 3808.1. Quantification of total crocins were carried out by collecting the peak areas of each crocin.

2.3. Preparation and characterization of feed solutions

Ethanol-water solution (80% ethanol) was used for dissolving zein at concentrations of 15, 25 and 30% w/v. Three grams of zein and different amounts of SE (0.15 g and 0.3 g) were dissolved in 10 ml ethanol-water solution, then solutions were stirred for 20 min at 600 rpm. These solutions were electrospun to obtain ZNLSE (5% and 10% wt, with respect to zein).

The electrical conductivity of the solutions was measured by a conductometer (WTW LF95, Germany).

The surface tension measurements of feed solutions were performed by the Wilhemy plate method using a tensiometer (Dataphysics DCAT 11 E, Germany).

The viscosity measurements of samples were conducted by using a rheometer (Haake Rheostress 1, Germany) equipped with a plate-plate sensor (dia = 35 mm, gap = 1 mm) at 25 °C. The shear rate range increased from 0.1 to 200 s^{-1} during 60 s. The data were modelled with the power law equation by using the software of the rheometer (Rheowin, Germany) as follows:

$$\tau = K\dot{\gamma}^{n} \quad (1)$$

where τ is the shear stress (Pa), K is the consistency index (Pa. s^n), n is the flow behavior index and $\dot{\gamma}$ is the shear rate (s^{-1}). After K and n values were obtained, then apparent viscosities (η) were calculated from the equation as follows:

$$\eta = K\dot{\gamma}^{n-1} \quad (2)$$

The maximum shear rate was calculated according Eq. (3) is given below, which is suitable for materials have power-law property in tubular geometry:

$$\dot{\gamma}_{max} = \left(\frac{3n+1}{4n}\right)\frac{4Q}{\pi R^3} \quad (3)$$

where Q is the volumetric flow rate of the material and R is the inside radius of the tube. The radius of the needle (inner diameter of 18-G needle is 0.838 mm) where feed solution coming out from it and exposed to the electric field was 0.419 × 10^{-3} m. The flow rate of the feed solution for this study was 0.8 mL/h, which is equal to Q = 2.22 × 10^{-10} m^3 s^{-1}. Then, the maximum shear rates values were calculated according to Eq. (3). The apparent viscosities were calculated from Eq. (2). at the corresponding maximum shear rate values (Table 1) (Okutan et al., 2014).

2.4. Electrospinning

The plastic syringe was filled with feed solution and placed into a syringe pump (New Era Pump Systems Inc., NE-300, USA). The voltage was applied by an external power supply (Nanofen, Ankara, Turkey). The distance between the tip of the needle and the collector plate was 15 cm and the flow rate was 0.8 mLh^{-1}. The electrospun samples were produced at voltages of 6 kV and 14 kV and collected on aluminum foils, which was used for covering the collector plate. ZNLSE containing 10% SE produced at 6 kV, was selected to use for further analysis.

2.5. Characterization of fibers

2.5.1. Morphology of electrospun samples

The nanofibrous surface morphology including the diameter was analyzed using a scanning electron microscope (SEM) Tescan Vega3 (USA) at 20.00 kV. Images are recorded at magnification ranges of 1 to 15000x. Then, the average fiber diameters were calculated using at least 100 randomly selected fibers diameter values using Image J software.

2.5.2. Differential scanning calorimetry (DSC)

DSC curves of samples were recorded by using a Differential Scanning Calorimeter (DSC Q10, New Castle, USA). The amount of 5 mg of each sample was weighted carefully in aluminum pans and hermetically sealed. An empty pan was used as a reference. The samples were heated from 26 °C to 196 °C at 10 °C min^{-1} under nitrogen atmosphere (50 mL min^{-1}).

2.5.3. ATR-FTIR characterization of electrospun samples

The infrared spectra of samples were gathered using a Fourier transformed infrared (ATR-FTIR) spectrometer (Bruker Model, Tensor II). OPUS program software from Bruker GmbH was used for data acquisition. IR spectra were recorded at a resolution of 2 cm^{-1} and 16 scans were done for each spectrum and the scanning range was between 4000 and 400 cm^{-1}.

2.5.4. Encapsulation efficiency

To determine the encapsulation efficiency (EE) of total crocins and

Table 1
The Conductivities, surface tensions, consistency indexes, flow behavior indexes, fluid behaviors and apparent viscosities of the zein and SE loaded zein solutions.

Solutions	Zein%[a]	SE% [b]	Conductivity (μS/cm)	Surface tension (mN/m)	K (Pa.s^n)	n (−)	Maximum shear rate	η (Pa.s) at max shear rate
Zein	15	–	1128±2^c	27.07 ± 0.06^b	0.05 ± 0.00^e	0.81 ± 0.04^c	4.07 ± 0.05^a	0.04 ± 0.00^e
Zein	25	–	1271±4^b	27.26 ± 0.11^a	0.09 ± 0.00^d	0.96 ± 0.02^b	3.89 ± 0.02^b	0.08 ± 0.00^d
Zein	30	–	1281±3^a	27.28 ± 0.04^a	0.12 ± 0.01^c	0.97 ± 0.02^b	3.88 ± 0.02^b	0.11 ± 0.01^c
Zein-SE	30	5	1269±4^b	26.83 ± 0.11^c	0.14 ± 0.01^b	1.09 ± 0.03^a	3.77 ± 0.03^c	0.16 ± 0.00^b
Zein-SE	30	10	1263±1^b	27.14 ± 0.05^{ab}	0.17 ± 0.01^a	1.05 ± 0.01^a	3.80 ± 0.01^c	0.19 ± 0.00^a

Data are displayed in means ± standard deviation of three replications. Values in each column with different letters were statistically significant ($p < 0.05$).
[a] With respect to solvent (ethanol/water, 8:2).
[b] With respect to zein polymer.

picrocrocin in the se, 10 mg of the sample was dissolved in ethanol 80% (v/v), and the concentrations of SE components in dissolved nanofiber solution was measured by HPLC. For assessment of the amount of SE components on the surface of the nanofibers (free compounds), The ZNLSEs was rinsed with distilled water (Alehosseini et al., 2019) and then the solution filtered by a 0.2 μm (millipore) filter, finally the crocins and picrocrocin content of filtered solution were determined by HPLC. The difference between the amounts of total and free compound was used to calculate the amount of the compound encapsulated in fibers. Finally, the encapsulation efficiency of crocins and picrocrocin were separately calculated according to Eq. (4).

$$EE\ \% = \frac{\text{SE compound encapsulated in } \textit{the fibers}}{\text{Therotical } \textit{SE compound in the fibers}} \times 100 \quad (4)$$

2.6. Determination of antioxidant activity by ABTS assay

The AA of saffron extract (SE), ZN, and ZNLSE containing 10% SE (containing equivalent amount of SE) were measured. For ZNLSE, 10 mg of nanofiber samples were dissolved in 5 mL of ethanol solution (% 80), then they were stirred at 500 rpm for 15 min. SE solution at concentration of 0.2 mg mL^{-1} in ethanol solution was also prepared. AA of solutions were determined using ABTS assay as stated by Bhatt et al. (2012) as described in supplementary material (p.6).

2.7. Treatment of fish fillets with ZNLSE

At first, the skins of fresh fish samples were removed and then they were filleted. The portioned (50 ± 2 g) fillets were randomly separated according to the sampling days and treatment groups defined for performing chemical analysis (Section 2.8). The electrospinning process was performed for 1 h to obtain equivalent amount of nanofiber mats for coating of defined samples. The fillets were coated with ZNLSE by rubbing to the surface of fish fillets as shown in supplementary material (Fig. S2). Both control (coated by aluminum foil without ZNLSE) fih samples and fish samples coated with ZNLSE were stored at 2 ± 1 °C for 8 days.

2.8. Physicochemical analysis

The different chemical indicators for fish deterioration were estimated, including the total volatile basic nitrogen (TVBN, expressed as mg N/100 g fish) using distillation method (Ceylan et al., 2017) and the thiobarbituric acid reactive substances (TBARS, expressed as mg malonaldehyde equivalent/kg fish) with the distillation method described by Crackel et al. (1988). More details of these methods and also the photogeraphic images can be found in supplimentary material (p.7-8, Fig. S3). Furthuremore, to understand the degradation of the lipids in fish samples, they were extracted using chloroform (see supplementary material) and the extracted phase which containing oil was used to determine PV and FFA according to the method described by Özogul et al. (2016) with slight modifications. The detailed explanation for these methods with the images of different steps are provided in supplimentary material (p.9, Fig. S4). The pH of fish samples was determined after homogenizing in distilled water (1:10 w/v) using a digital pH meter (WTW pH 330i Taschen pH Meter; WTW GmbH).

2.9. Statistical analysis

The experiments were done in triplicate and the results were reported as mean ± standard deviation. The variances between means were analyzed using SPSS 25.0 software (SPSS Inc., Chicago, IL, USA). Differences between means were considered significant at $p < 0.05$. Duncan's test was used to compare mean values. For physicochemical analysis, significant differences between two groups of treatments were determined through two-sided t-tests (means test of equality) at the 95% significance level ($p < 0.05$) using SPSS 25.0 Statistics software.

3. Results and discussion

3.1. Properties and electrospinnability of feed solutions

The electrical conductivities, surface tensions, and rheological results of feed solutions are presented in Table 1. Non-zero electrical conductivity is required and low surface tension is preferred for electrospinning (Moradkhannejhad et al., 2018).

The electrical conductivities of the solutions increased significantly with zein concentration. The formation of the Taylor cone can be accelerated when a solution with high electrical conductivity is used for electrospinning (Dehcheshmeh & Fathi, 2019). However, the conductivity of the 30% zein solution decreased with the addition of SE ($p < 0.05$). Joukar (2012) examined the electrophysiological conduction of rat heart and reported that higher doses of SE significantly slowed the electrical conductivity of the heart. Therefore, SE may have ability to reduce the electrical conductivity. Low electrical conductivity (high conductivity being considered as >10 mS/cm) is preferable for nanofiber formation since the feeding solution is subjected to weaker electrical forces (Moradkhannejhad et al., 2018). A decrease in the conductivity of the solution could also reduce beading as a result of less stretching of the polymer jets, which tends to produce thicker nanofibers (Aslaner et al., 2021; Facchi et al., 2021). This was the case in our study, as seen in Table S1. As electrical conductivity decreased, thicker fibers were obtained.

The surface tension values of the solutions increased with zein concentration ($p < 0.05$). The addition of SE decreased the surface tension of the feed solutions. The low surface tension values of the feed solutions at 26.83–27.28 mN m^{-1} compared to the surface tension of water at ~72 mN m^{-1} enabled them to be electrospun. The low surface tension of the solutions was probably due to the presence of ethanol (~22 mN m^{-1}).

The electrical field strength values for the electrospinning process were 6 kV/15 cm = 0.40 kV/cm and 14 kV/15 cm = 0.93 kV/cm. As surface tension decreases, the required electrical field strength for jet initiation during electrospinning also decreases. Electrical conductivity and surface tension have counter-effects on electrospinning; namely, low electrical conductivity requires high electric field strength whereas low surface tension requires low electric field strength for jet initiation. (Kriegel et al., 2009). In the present study, feed solutions containing

15% and 25% zein with relatively high electrical conductivity and low surface tension could be electrospun at lower electrical field strength; however, it appears that the zein concentration prominently affected the process.

According to the results, the feed solutions displayed non-Newtonian behavior. The feed solutions without SE exhibited pseudoplastic behavior, whereas solutions containing SE were dilatant. The calculated apparent viscosity values increased with zein concentration and the additions of SE. Dehcheshmeh (2019) reported that higher viscosity of feed solution may promote fabrication of thicker nanofibers as a result of the acceleration of the process. Our results (Table S1) were in accordance with the previously published data.

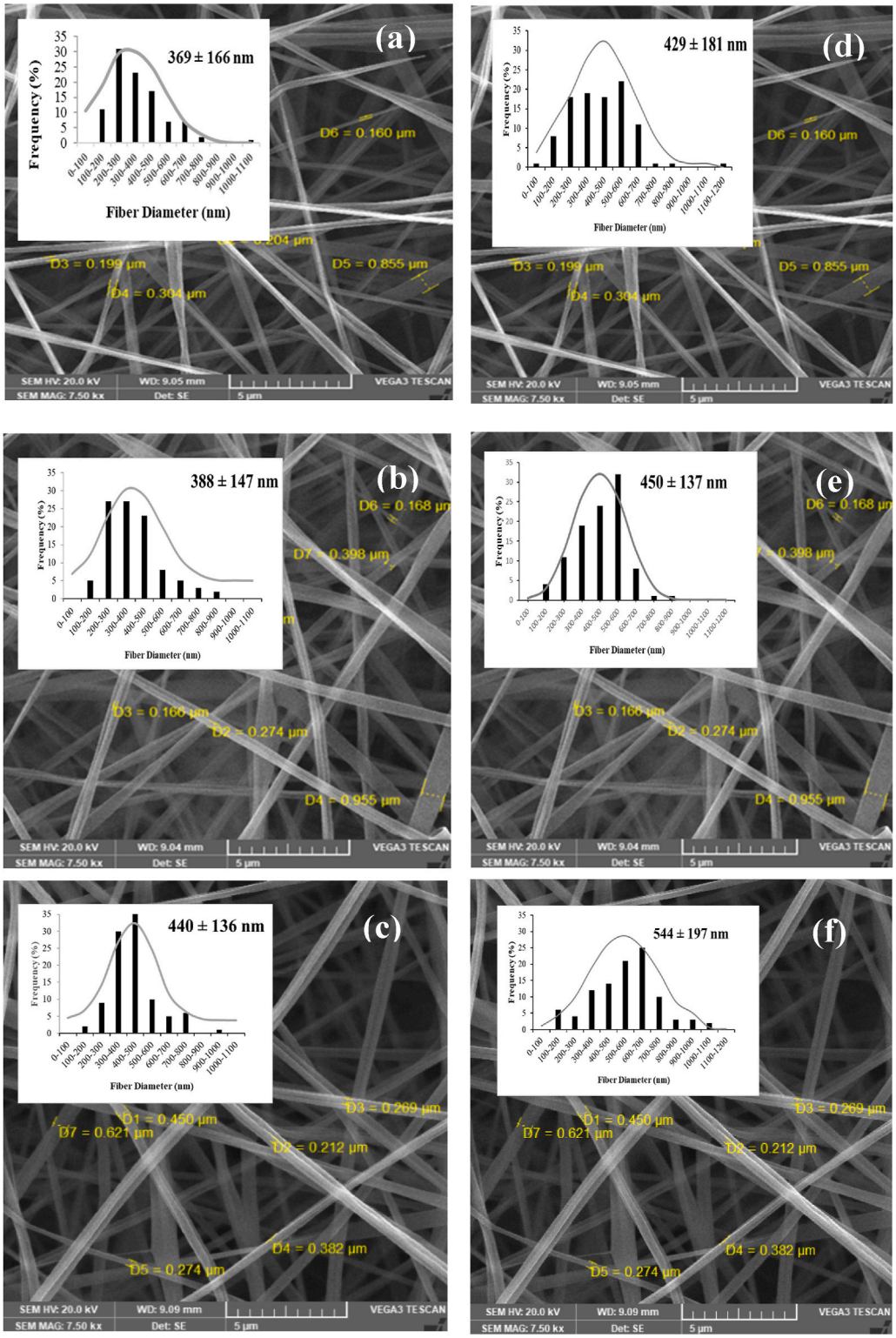

Fig. 1. SEM images and diameter distributions of electrospun mats obtained at 6 kV: 30% (w/v) zein polymer solution loaded with SE contents at (a) 0%, (b) 5%, and (c) 10% (w/w) and SEM images and diameter distributions of electrospun fibers obtained at 14 kV: from 30% (w/v) zein polymer solutions with SE contents at (d) 0%, (e) 5% and (f) 10% (w/w). Magnification is 7500 × .

3.2. Characterization studies

3.2.1. Morphology of fibers

The SEM images of ZNs obtained by the electrospinning of various concentrations of zein are shown in Supplementary Fig. S1. Spherical droplets containing very rare fibers were seen to result from the electrospinning of zein 15% (w/v) solution. This is probably due to low viscosity as a result of lower zein contents compared to other solutions. If polymers are insufficiently entangled, beads or droplets can occur during electrospinning (Kriegel et al., 2009). Fibers were successfully formed at the 25% concentration of zein but were found to have beads. Chang et al. (1999) reported that insufficient zein concentrations cause the formation of beads due to the fact that Rayleigh instability cannot be avoided. Beadless, smooth, and ultrafine nanofibers were obtained from the zein solution at 30% w/v. The fiber diameter increased with zein concentration (Table S1). Zein solutions with higher concentrations had higher viscosities, which is not favorable due to the "bending instability" phenomenon. Therefore, reduction in jet path due to less stretching of the feed solution resulted in the formation of fibers with larger diameters during the electrospinning of zein solutions with higher concentrations (Ramakrishna et al., 2005).

Fiber diameter histograms and SEM images of ZNs containing 30% zein in terms of SE addition and varying applied voltages are presented in Fig. 1. The fiber diameter increased significantly with the addition of 10% SE ($p < 0.05$). Increasing in diameters may be caused by interactions between bioactive components and zein, which will further lead to a decrease in the polyelectrolyte character of a biopolymer solution. This also decreases the repulsion between the polycationic protein chains. Similarly, Antunes et al. (2017) reported that the addition of eucalyptus essential oil/cyclodextrin to zein solutions increased fiber diameter. In the present study, fiber diameter increased with the applied voltage (Fig. 1 and Table S1). Fiber diameter is usually expected to decrease with increasing voltage, but thicker fibers were formed at a voltage of 14 kV. Since higher voltages create stronger electric fields, the repulsion charges of the jet increase and that leads to greater stretching of the jet formation of thinner fibers. Increases in nanofiber diameter may also happen due to accelerations in polymer solution motions. Therefore, it is assumed that increasing voltages with stronger electric fields may be able to draw bigger droplets from feeding solutions and the average fiber diameter could thus be larger than that of fibers obtained at lower voltages (Alehosseini et al., 2019; Zhu et al., 2017).

3.2.2. Thermal properties

The DSC thermograms for SE in pure form, zein powder, ZNs, and encapsulated SE at 5% and 10% within ZNs are shown in Fig. 2. The ZN denaturation transition was observed as an endothermic peak at 127.66 ± 0.72 °C. Many endothermic peaks were detected for SE because it has many bioactive compounds. The sharp peak detected at 145.74 ± 0.60 °C may correspond to the melting point of picrocrocin (Garavand et al., 2019). After the combination of zein and SE, the endothermic peaks of 5% and 10% ZNLSE complexes were decreased to 118.7 ± 3.64 °C and 108.2 ± 4.70 °C, respectively. It can be concluded that the distribution of SE in the zein polymer matrix may result in diminished thermal stability of the ZNLSE due to its hydrophilicity. In the DSC curve of the ZNLSE, no sharp endothermic peak appeared, which may confirm that the SE exists in an amorphous form rather than a crystalline form. It may also indicate the presence of bonding between zein and SE molecules with the formation of a compact structure (Chen et al., 2019).

3.2.3. FTIR spectroscopy

The infrared spectra of pure zein powder, SE, ZNs, and 10% ZNLSE are given in Fig. 3. The spectrum of the pure zein powder revealed absorbance bands of lowest peak intensities for –NH and –OH groups at 3294 cm^{-1}, carboxylic acids at 2925 cm^{-1}, amide I (C═O stretching) at 1647 cm^{-1}, amide II (N–H bending) at 1515 cm^{-1}, amide III (C–N stretching) at 1241 cm^{-1}, and C–N stretching at 1452 cm^{-1}

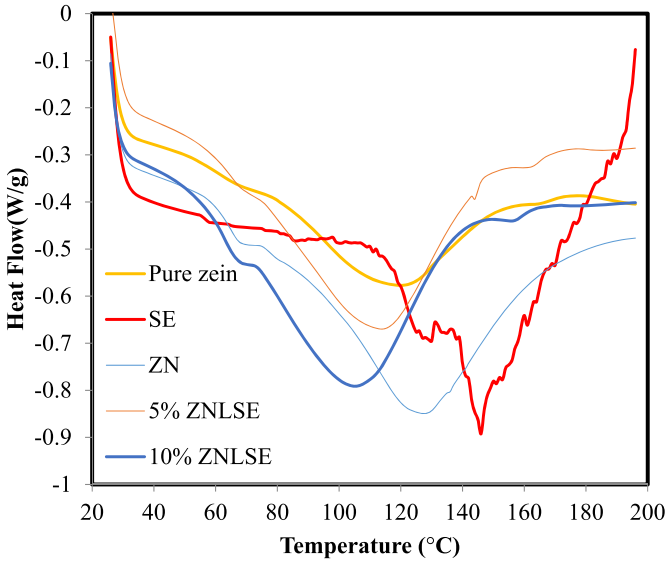

Fig. 2. DSC profiles (heat flow versus temperature) of pure zein powder, SE, ZN and ZNLSE.

(Dehcheshmeh & Fathi, 2019).

The characteristic peaks of SE appeared at 3294 cm^{-1}, 2924 cm^{-1}, 1608 cm^{-1}, 1577 cm^{-1}, 1269 cm^{-1}, 1224 cm^{-1}, 1163 cm^{-1}, 1017 cm^{-1}, and 747 cm^{-1}. The peak at 3292 cm^{-1} was attributed to the O–H of sugar groups existing in the structure of crocin (Alehosseini et al., 2019). The wide peak between 2921 and 2880 cm^{-1} exhibits symmetric $–CH_3$ and $–CH_2$ stretching vibrations and asymmetric $–CH_2$ stretching vibrations. The bands at 1608 cm^{-1} and 1577 cm^{-1} indicate the asymmetric and symmetric stretching peaks of carboxylic groups (C═C stretching). Furthermore, at 1608 cm^{-1} (C═O stretching), ester and ketone groups connected to an aromatic ring chain were observed (Dehcheshmeh & Fathi, 2019). The peak observed at 1269 cm^{-1} represents the C–C–C bonding and C–C–H bonding of the aromatic groups of SE components. The peak at 1224 cm^{-1} was attributed to the C–O stretching vibrations of the cyclic ether groups. The band at 1163 cm^{-1} matches the CCH bonding from the aromatic rings and the C–O–C in-plane bending of the inter-ring chain. The peaks at 1017 cm^{-1} and 747 cm^{-1} are due to the –CH in-plane bending of the aromatic rings connected to the ortho and meta directing groups.

The characteristic bands of zein were observed at 1652 cm^{-1} (amide I), 1544 cm^{-1} (amide II), 1241 cm^{-1} (amide III), and 1453 cm^{-1} related to C═O stretching vibrations, N–H in-plane bending, C–N stretching vibrations, and C–N stretching vibrations, respectively. The stretching of –NH and –OH groups and C–H stretching vibrations of aliphatic ($–CH_2$ and CH_3) groups were revealed at 3294 cm^{-1} and 2930 cm^{-1}, respectively (Cetinkaya et al., 2022; Liu et al., 2018).

The FTIR spectra of ZNLSE had characteristic peaks at ~3294 cm^{-1}, 2958 cm^{-1}, 2931 cm^{-1}, 1650 cm^{-1}, 1541 cm^{-1}, and 1450 cm^{-1}. There were differences in peak assignments for ZNLSE compared to ZNs; first, the amplitude of a peak with wavenumber between 3600 and 3100 cm^{-1} (representing –NH, –CH, and mainly –OH groups) was observed in the spectrum of ZNLSE. In other words, the peak transmittance intensity at 3293 cm^{-1} was greatly strengthened for ZNLSE compared to the same peak for the ZN spectrum. The characteristic band revealed electrostatic interaction between zein and SE. Secondly, the carbonyl-amide region between 1650 and 1450 cm^{-1} changed in the ZNLSE spectrum. The characteristic transmittance of amide I groups at 1652 cm^{-1} in the ZN spectrum shifted slightly to 1650 cm^{-1}, while the transmittance of amide II groups in the ZN spectrum shifted slightly from 1544 cm^{-1}–1541 cm^{-1} for the ZNLSE spectrum (Liu et al., 2018). It is assumed that the carboxyl group (−COO) of the SE may interact with the amino group ($-NH_2$) of zein and form an ionic complex. Thirdly, peaks

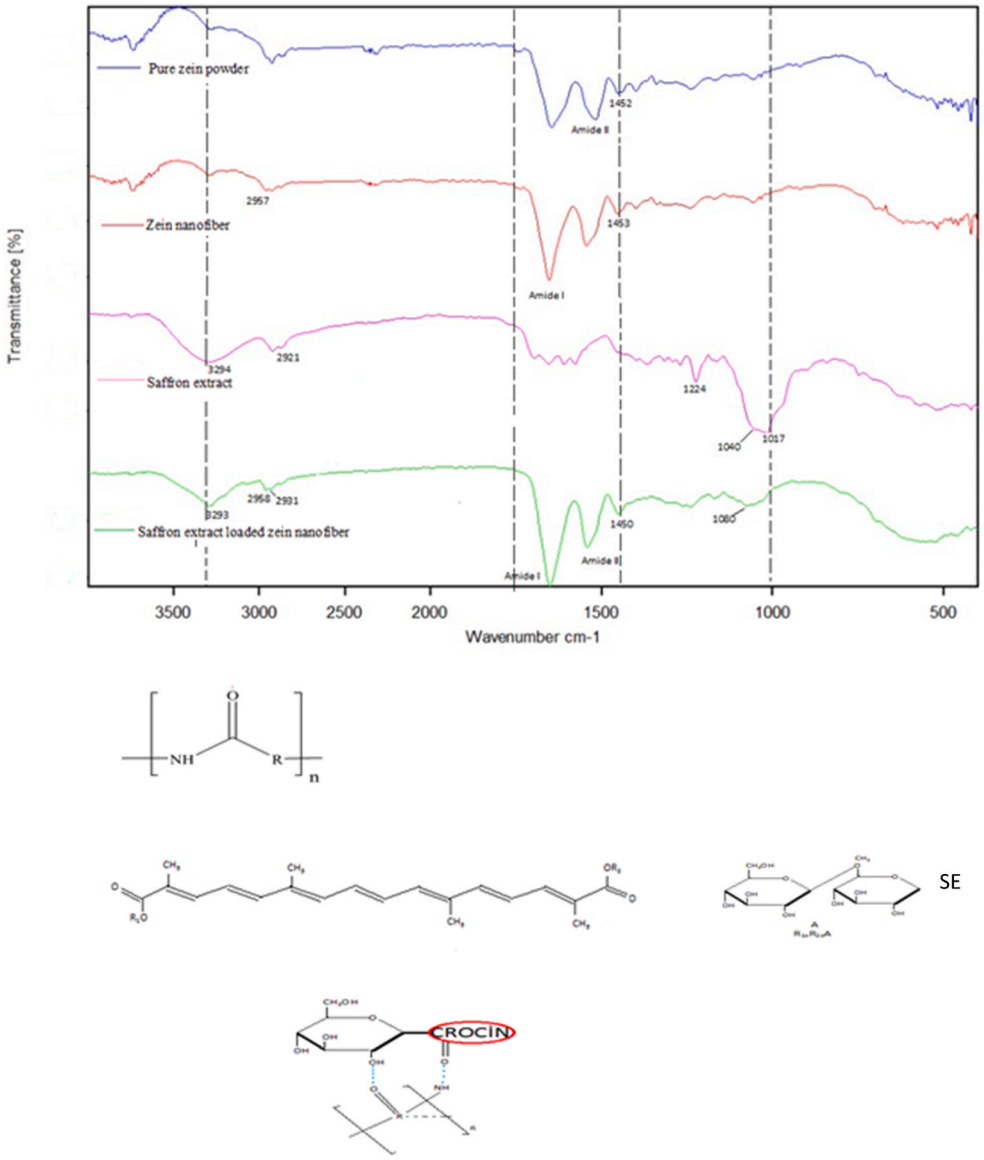

Fig. 3. ATR-FTIR spectra of pure zein powder, SE, Zein nanofiber (ZN) and Zein nanofiber loaded with SE 10% (ZNLSE).

corresponding to the vibrations of aromatic rings and an inter-ring chain (1608 cm^{-1}, 1577 cm^{-1}, 1364 cm^{-1}, 1316 cm^{-1}, 1292 cm^{-1}, 1269 cm^{-1}, and 747 cm^{-1}) that were present in the SE spectrum completely disappeared in the ZNLSE spectrum. These disappearing peaks were related to vibrations of C–C–C (the C–C stretching vibration of SE was restricted after encapsulation), C–C–H, and C–O–C of aromatic rings and the inter-ring chain of native SE. These results confirm the interactions of hydrophobic and hydrogen bonding among zein proteins and SE. The results were in accordance with the findings of Tarantilis et al. (1998), who revealed that the "fingerprint" (1100 cm^{-1} to 1400 cm^{-1}) might be the key band for structural and conformational changes of conjugated double bond systems in saffron plant.

Furthermore, there was a shift of the amide bands to a region of lower wavenumber for the ZNLSE spectrum. Antunes et al. (2017) reported in their study that the peaks of amide I and amide II depend on the size of the α-helix structure and a lower wavenumber suggests greater structural stability, which is related to the increased H bonding occurring at the N–H group. Finally, the "fingerprint" that appeared for the shoulder band of ZNLSE at 1080 cm^{-1} (seen at 1040 cm^{-1} for SE) revealed that the structural conformation of SE was not broken after interacting with zein proteins (Zhang et al., 2019). Based on the points explained here, it can be concluded that nanoencapsulation of SE was achieved successfully.

3.2.4. *Encapsulation efficiency*

The encapsulation efficiencies of total crocins and picrocrocin in ZNLSE (10% SE) were 63.9 ± 0.2% and 47.6 ± 0.1%, respectively. Alehosseini et al. (2019) produced both electrosprayed particles and electrospun fiber structures from zein solutions incorporated with SE at different concentrations. Their results, obtained via spectrophotometric method, revealed that the EE of the crocins in zein fibers decreased from 97% to 80% with the increasing of SE loading from 2% to 4%, respectively. In the present study, at 10% SE loading, the EE of the crocins was reduced even more (64%). This could be attributed to the increasing component/wall material ratio in the encapsulation systems.

The HPLC chromatograms for SE and ZNLSE (10%) are presented in Fig. 4. Peaks related to *trans*-crocin-4, *trans*-crocin-3, and *cis*-crocin-3 were identified in SE and electrospun samples dissolved in water to measure the unencapsulated components (Fig. 4 b1). For determination of the levels of both encapsulated and free components, the electrospun fibers were dissolved in ethanol (80%) and the resulting chromatogram of that sample is shown in Fig. 4(b2).

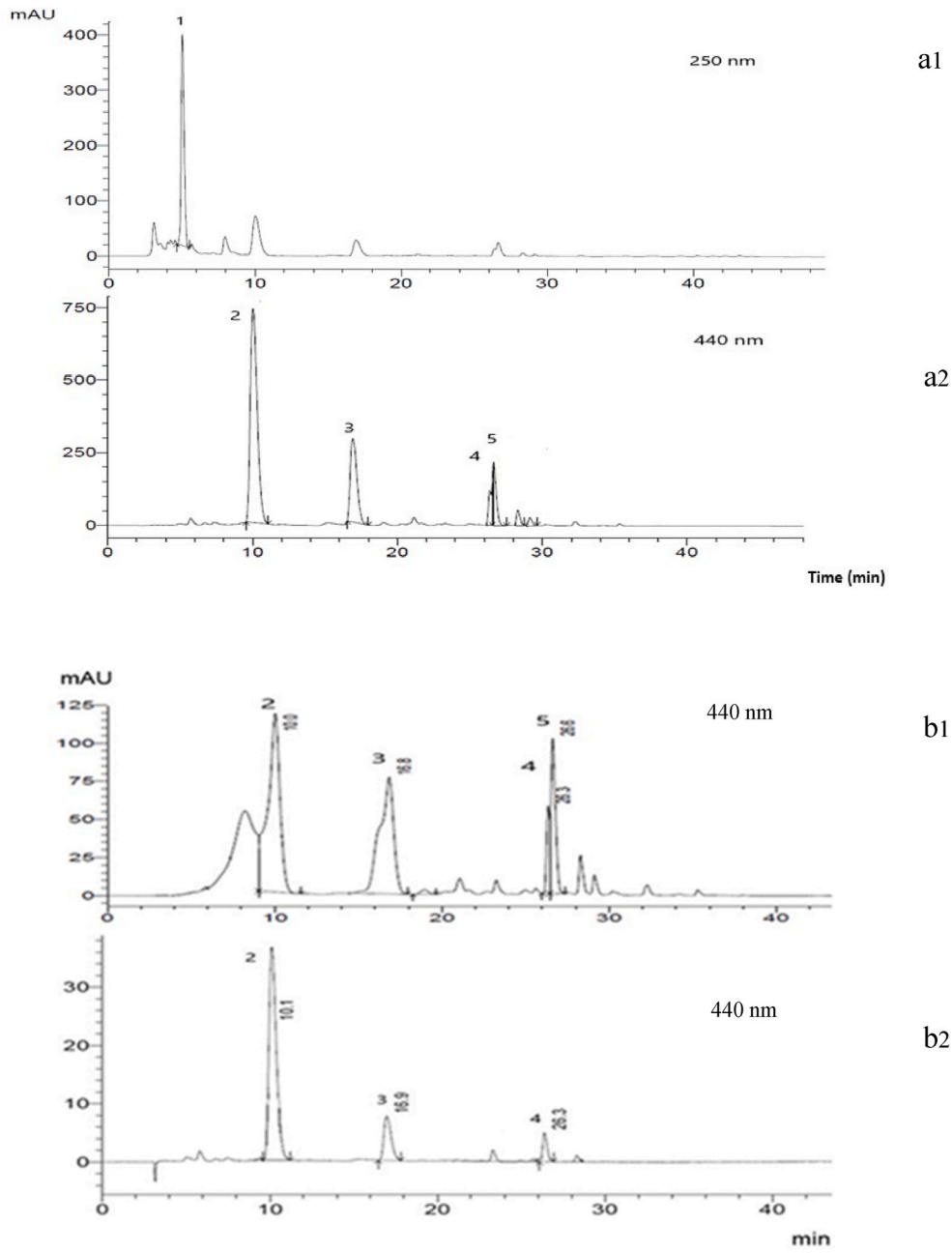

Fig. 4. HPLC-DAD profiles of the RP separation of (1) picrocrocin at 250 nm and crocins at 440 nm from a representative saffron extract at concentration of 1 mg mL^{-1} (a1 and a2) and from ZNLSE (10%) (b1) total crocins and (b2) sample rinsed with water (free crocins).The identified peaks are (1) Picrocrocin (2) *trans*-crocin-4, (3) *trans*-crocin-3, (4) *cis*-crocin-4, (5) *cis*-crocin-3 with the retention times of 5.0, 10.0, 16.9, 26.3 and 26.9 min, respectively.

3.3. Antioxidant activity

The AA of a coating material determines its ability to limit the oxidation of food products. The AA of pure ZN was 31.6 ± 1.9%. Similar values were found by other researchers for the AA of pure ZN. The inhibition of ABTS free radicals by ZN can be explained by the high surface area of the nanofibers, which provides more contact with the solution containing free radicals. Moreover, the presence of α-zein in the nanofibers contributes to the AA (Altan et al., 2018; Aytac et al., 2016; Aman Mohammadi et al., 2021). SE showed AA of 17.5 ± 1.3%, which could be due to the presence of bioactive constituents, particularly crocin, kaempferol, and phenolic components (Popović-Djordjević et al., 2021). Interestingly, after the encapsulation of SE (10%) into ZNs, the AA of ZNLSE rose to 56.3 ± 5.8%. These findings revealed that the combination of SE and ZN showed a synergistic effect. This effect could be attributed to the nanoencapsulation of SE components, providing a stronger contribution to the AA. Moreover, interactions between the free amino groups (NH_2) of zein and the carboxyl group of SE may form more stable radical molecules, which could avoid oxidation.

3.4. Chemical analysis of fish samples

In the present study, the total volatile basic nitrogen (TVBN) contents in fish meat at the end of storage should not exceed the level of 35 mg/100 g (Ceylan et al., 2017). The TVBN levels of control and ZNLSE-treated samples were below that limit value until the end of the storage period (Table 2). TVBN values for samples coated with ZNLSE were lower than those obtained for control samples. Baygar and Alparslan (2015) noted that TVBN values for fillets of seabass stored at 4 ± 2 °C were found to be 18.11, 21.61, and 23.70 mg/100 g on the 0, 2nd,

Table 2
Changes in physicochemical properties of 10% ZNLSE-coated and uncoated sea bass fillets during refrigerated storage (2 °C).

TVBN (mg/100g)	Day 0	Day 2	Day 4	Day 6	Day 8
Control	18.10 ± 1.54^{d}	21.76 ± 0.16^{bcA}	19.88 ± 2.11^{cdA}	24.03 ± 1.17^{bA}	28.56 ± 0.00^{aA}
Coated Fish Samples	18.10 ± 1.54^{a}	17.83 ± 0.16^{aB}	18.76 ± 2.67^{aA}	19.41 ± 0.58^{aB}	19.97 ± 0.43^{aB}
TBARS (mg MDA/kg)					
Control	3.42 ± 0.58^{b}	5.49 ± 0.14^{aA}	5.61 ± 0.59^{aA}	2.53 ± 0.22^{cA}	2.38 ± 0.26^{dA}
Coated Fish Samples	3.42 ± 0.58^{abB}	2.66 ± 0.31 ^{bB}	4.12 ± 0.7^{aB}	1.04 ± 0.15^{cB}	1.04 ± 0.22^{cB}
PV (meq O2/kg)					
Control	1.3 ± 0.09^{e}	2.57 ± 0.15^{dA}	3.6 ± 0.05^{cA}	4.4 ± 0.13^{aA}	3.88 ± 0.03^{bA}
Coated Fish Samples	1.3 ± 0.09^{d}	1.95 ± 0.05^{cB}	3.00 ± 0.05^{bB}	3.05 ± 0.05^{bB}	3.27 ± 0.08^{aB}
Free Fatty Acid (%)					
Control	0.16 ± 0.01^{e}	0.27 ± 0.01^{dA}	0.36 ± 0.02^{cA}	0.42 ± 0.03^{bA}	0.55 ± 0.01^{aA}
Coated Fish Samples	0.16 ± 0.01^{e}	0.18 ± 0.01^{dB}	0.22 ± 0.01^{cB}	0.31 ± 0.02^{bB}	0.35 ± 0.02^{aB}
pH					
Control	6.31 ± 0.05^{d}	6.27 ± 0.08^{cdA}	6.38 ± 0.02^{cA}	6.78 ± 0.02^{bA}	7.10 ± 0.03^{aA}
Coated Fish Samples	6.31 ± 0.05^{a}	6.29 ± 0.08^{abA}	6.13 ± 0.03^{dB}	6.15 ± 0.01^{cdB}	6.22 ± 0.02^{bcB}

Data are displayed in means ± standard deviation of three replications.
$^{a-e}$Within each row, different superscript lowercase letters show differences between different storage days ($p < 0.05$).
$^{A-B}$ Within each column superscript upercase letters show differences between different treatment groups ($p < 0.05$).

and 6th day, respectively. In the present study, TVBN values of 19.97 and 28.56 mg/100 g were obtained for ZNLSE-treated and uncoated samples on the 8th day of storage. Lower values of TVBN for the coated groups on different days of storage indicated that ZNLSE was successful in preventing the rapid increase of TVBN values.

The content of thiobarbituric acid reactive substances (TBARS) is an important indicator when evaluating the degree of lipid oxidation in meat products (Zheng et al., 2022). On the initial day, the TBARS value of the control sample was 3.42 mg MDA/kg. The TBARS values obtained for ZNLSE-coated samples and control group samples on the last day of storage were 1.04 mg MDA/kg and 2.38 mg MDA/kg, respectively.

The TBARS values reached to maximum point at 4th day of storage and then decreased. The simillar trend was obsereved in other studies (Thiansilakul et al., 2010; Zhou et al., 2019; Özogul et al., 2016). MDA is an intermediate by-product generated during lipid oxidation and it can be further oxidized to other oxidation products such as organic acids and alcohols. These compounds do not react with TBA and this might be the reason for decreasing TBARS values during storage period. On the other hand, as can be seen from Table 2, the TBARS values of ZNLSE-coated samples were significantly lower than those of the control group samples during storage ($p < 0.05$). Aboutorab et al. (2021) also found that the TBARS values of control shrimp samples were higher compared to shrimp dipped into SE-loaded nanoemulsions.

PV analysis was performed to measure the concentration of the primary oxidation products (hydroperoxides) during 8 days of refrigerated storage. The initial PV of control fillet was 1.3 ± 0.09 meq oxygen/kg of fish sample. PVs for un-coated fish fillets elevated continuously up to the amount of 4.4 ± 0.13 at the 4th day of storage and then decreased from day 6 to 8. The reason can be decomposition of hydroperoxide into other oxidation products during storage. The similar results have been found by Özogul et al. (2016) and Thiansilakul et al.(2010), who indicated the PVs of fish fillets decreased after reaching to a maximum value during cold storage. The PV of coated samples progressively increased throughout storage time and these samples had lower PV than control samples during storage days.

The initial FFA values of fish fillets was 0.16% of oleic acid, which was similar to that found by Ebadi et al. (2019). FFA value gradually increased in all samples over the time and reached to 0.55 and 0.35% oleic acid for control and coated fish samples after 8 days of storage, respectively. This increase can be related to the enzymatic hydrolysis of fish lipids. Our results also indicated that FFA value in the fish fillets coated with ZNLSE, was significantly lower than control group ($P < 0.05$). It can be probably due to the antimicrobial ability of the nanocoating material as can be proved by the results of TVBN and pH.

He and Xiao (2016) reported the range between 6.0 and 7.0 for pH values of fish fillets. The initial pH values of our sample was 6.31. The pH of control samples gradually increased and reached to 7.10 at day 8 during storage. The storage time had a significant effect on pH values of control samples ($P < 0.05$). However, its effect was not significant for coated samples during storage. During the storage period, the increase in pH can be due to the collection of alkaline compounds which generated by bacterial enzymes (Ebadi et al., 2019). Throughout whole storage period, the pH values of coated samples were significantly lower than that of the control sample ($P < 0.05$).

4. Conclusions

SE was successfully encapsulated into ZNs by electrospinning. Picrocrocin and four glycosyl esters of crocetin, namely *trans*-crocin-4, *trans*-crocin-3, *cis*-crocin-3, and *cis*-crocin-4, were detected in SE by LC-MS. A zein concentration of 30% w/v is necessary to form enough chain polymer entanglements to prevent the formation of bead morphologies. The diameters of the obtained fibers increased with SE concentration as well as applied voltage. Smoother beadless fibers were obtained from 30% zein solution containing 10% SE at 6 kV and 14 kV with average diameters of 440 nm and 544 nm, respectively. DSC profiles confirmed the change in the crystalline form of SE, which indicated the successful incorporation of SE molecules in the zein proteins. The ATR-FTIR graphs confirmed the disappearance of peaks because of secondary interactions, shifted signals, and in-plane bending of –OH groups in ZNLSE. The spectra confirmed the formation of hydrogen bonds between zein and SE in ZNLSE. Furthermore, interaction between the free amino groups (NH_2) of zein and the carboxyl group of SE components was associated with the high AA of 10% ZNLSE due to the production of more stable radical molecules. All of these results clarified the successful encapsulation of SE.

The findings of physicochemical analysis indicated that ZNLSE containing 30% zein and 10% SE has great potential to be used to extend the shelf life of seafood products and delay their spoilage during cold storage. The fabricated ZNLSE can be used as an antioxidant coating and active packaging material. Therefore, the protective effects of ZNLSE for food products should be examined further by additional analysis in future studies.

CRediT authorship contribution statement

Zahra Najafi: Data curation, Investigation, Formal analysis, Visualization, Validation, Writing – original draft, preparation, Writing – review & editing. **Turgay Cetinkaya:** Investigation, Formal analysis, Writing – original draft, Writing – review & editing. **Fatih Bildik:** Formal analysis, Writing – review & editing. **Filiz Altay:** Conceptualization, Project administration, Supervision, Resources, Methodology, Writing – review & editing. **Neşe Şahin Yeşilçubuk:** Project administration, Supervision, Resources, Writing – review & editing.

Declaration of interest

The authors declare that they have no known competing financial interests or personal relationships that could have appeared to influence the work reported in this paper.

Acknowledgments

This work was supported by the Research Fund of the Istanbul Technical University (Project no.:MDK- 2018- 41582). The study was designed as a part of Zahra Najafi's Ph.D. thesis (First advisor: Prof. Dr. Neşe Şahin-Yeşilçubuk, and co-advisor: Prof. Dr. Filiz Altay).

Appendix A. Supplementary data

Supplementary data to this article can be found online at https://doi.org/10.1016/j.lwt.2022.113588.

References

Aboutorab, M., Ahari, H., Allahyaribeik, S., Yousefi, S., & Motalebi, A. (2021). Nano-emulsion of saffron essential oil by spontaneous emulsification and ultrasonic homogenization extend the shelf life of shrimp (Crocus sativus L.). *Journal of Food Processing and Preservation, 45*(2), Article e15224. https://doi.org/10.1111/jfpp.15224

Ahmadian-Kouchaksaraie, Z., & Niazmand, R. (2017). Supercritical carbon dioxide extraction of antioxidants from Crocus sativus petals of saffron industry residues: Optimization using response surface methodology. *The Journal of Supercritical Fluids, 121*, 19–31. https://doi.org/10.1016/j.supflu.2016.11.008

Alehosseini, A., Gómez-Mascaraque, L. G., Ghorani, B., & López-Rubio, A. (2019). Stabilization of a saffron extract through its encapsulation within electrospun/electrosprayed zein structures. *LWT, 113*, Article 108280. https://doi.org/10.1016/j.lwt.2019.108280

Altan, A., Aytac, Z., & Uyar, T. (2018). Carvacrol loaded electrospun fibrous films from zein and poly(lactic acid) for active food packaging. *Food Hydrocolloids, 81*, 48–59. https://doi.org/10.1016/j.foodhyd.2018.02.028

Aman Mohammadi, M., Ramezani, S., Hosseini, H., Mortazavian, A. M., Hosseini, S. M., & Ghorbani, M. (2021). Electrospun antibacterial and antioxidant zein/polylactic acid/hydroxypropyl methylcellulose nanofibers as an active food packaging system. *Food and Bioprocess Technology, 14*(8), 1529–1541. https://doi.org/10.1007/s11947-021-02654-7

Ansarifar, E., & Moradinezhad, F. (2022). Encapsulation of thyme essential oil using electrospun zein fiber for strawberry preservation. *Chemical and Biological Technologies in Agriculture, 9*(1), 1–11.

Antunes, M. D., da Silva Dannenberg, G., Fiorentini, Â. M., Pinto, V. Z., Lim, L.-T., da Rosa Zavareze, E., & Dias, A. R. G. (2017). Antimicrobial electrospun ultrafine fibers from zein containing eucalyptus essential oil/cyclodextrin inclusion complex. *International Journal of Biological Macromolecules, 104*, 874–882. https://doi.org/10.1016/j.ijbiomac.2017.06.095

Armellini, R., Peinado, I., Pittia, P., Scampicchio, M., Heredia, A., & Andres, A. (2018). Effect of saffron (Crocus sativus L.) enrichment on antioxidant and sensorial properties of wheat flour pasta. *Food Chemistry, 254*, 55–63. https://doi.org/10.1016/j.foodchem.2018.01.174

Aslaner, G., Sumnu, G., & Sahin, S. (2021). Encapsulation of grape seed extract in rye flour and whey protein–based electrospun nanofibers. *Food and Bioprocess Technology, 14*(6), 1118–1131.

Aytac, Z., Kusku, S. I., Durgun, E., & Uyar, T. (2016). Encapsulation of gallic acid/cyclodextrin inclusion complex in electrospun polylactic acid nanofibers: Release behavior and antioxidant activity of gallic acid. *Materials Science and Engineering: C, 63*, 231–239. https://doi.org/10.1016/j.msec.2016.02.063

Baygar, T., & Alparslan, Y. (2015). Effects of multiple freezing (-18 ± 2 °C) and microwave thawing cycles on the quality changes of sea bass (Dicentrarchus labrax). *Journal of Food Science & Technology, 52*(6), 3458–3465. https://doi.org/10.1007/s13197-014-1373-z

Bhatt, I. D., Dauthal, P., Rawat, S., Gaira, K. S., Jugran, A., Rawal, R. S., & Dhar, U. (2012). Characterization of essential oil composition, phenolic content, and antioxidant properties in wild and planted individuals of Valeriana jatamansi Jones. *Scientia Horticulturae, 136*, 61–68. https://doi.org/10.1016/j.scienta.2011.12.032

Bhat, N. A., Wani, I. A., Hamdani, A. M., & Gani, A. (2021). Development of functional cakes rich in bioactive compounds extracted from saffron and tomatoes. *Journal of Food Science & Technology*. https://doi.org/10.1007/s13197-021-05267-2

Cetinkaya, T., Mendes, A. C., Jacobsen, C., Ceylan, Z., Chronakis, I. S., Bean, S. R., & García-Moreno, P. J. (2021). Development of kafirin-based nanocapsules by electrospraying for encapsulation of fish oil. *LWT, 136*, Article 110297.

Cetinkaya, T., Wijaya, W., Altay, F., & Ceylan, Z. (2022). *Fabrication and characterization of zein nanofibers integrated with gold nanospheres*. LWT, Article 112976.

Ceylan, Z., Sengor, G. F. U., & Yilmaz, M. T. (2017). A novel approach to limit chemical deterioration of gilthead sea bream (sparus aurata) fillets: Coating with electrospun nanofibers as characterized by molecular, thermal, and microstructural properties. *Journal of Food Science, 82*(5), 1163–1170. https://doi.org/10.1111/1750-3841.13688

Chang, H.-C., Demekhin, E. A., & Kalaidin, E. (1999). Iterated stretching of viscoelastic jets. *Physics of Fluids, 11*(7), 1717–1737. https://doi.org/10.1063/1.870038

Chen, S., Han, Y., Wang, Y., Yang, X., Sun, C., Mao, L., & Gao, Y. (2019). Zein-hyaluronic acid binary complex as a delivery vehicle of quercetagetin: Fabrication, structural characterization, physicochemical stability and in vitro release property. *Food Chemistry, 276*, 322–332. https://doi.org/10.1016/j.foodchem.2018.10.034

Crackel, R. L., Gray, J. I., Pearson, A. M., Booren, A. M., & Buckley, D. J. (1988). Some further observations on the TBA test as an index of lipid oxidation in meats. *Food Chemistry, 28*(3), 187–196. https://doi.org/10.1016/0308-8146(88)90050-7

Dehcheshmeh, M. A., & Fathi, M. (2019). Production of core-shell nanofibers from zein and tragacanth for encapsulation of saffron extract. *International Journal of Biological Macromolecules, 122*, 272–279. https://doi.org/10.1016/j.ijbiomac.2018.10.176

Ebadi, Z., Khodanazary, A., Hosseini, S. M., & Zanguee, N. (2019). The shelf life extension of refrigerated Nemipterus japonicus fillets by chitosan coating incorporated with propolis extract. *International Journal of Biological Macromolecules, 139*, 94–102. https://doi.org/10.1016/j.ijbiomac.2019.07.204

Facchi, D. P., Souza, P. R., Almeida, V. C., Bonafe, E. G., & Martins, A. F. (2021). Optimizing the Ecovio® and Ecovio®/zein solution parameters to achieve electrospinnability and provide thin fibers. *Journal of Molecular Liquids, 321*, Article 114476.

Garavand, F., Rahaee, S., Vahedikia, N., & Jafari, S. M. (2019). Different techniques for extraction and micro/nanoencapsulation of saffron bioactive ingredients. *Trends in Food Science & Technology, 89*, 26–44. https://doi.org/10.1016/j.tifs.2019.05.005

He, Q., & Xiao, K. (2016). The effects of tangerine peel (Citri reticulatae pericarpium) essential oils as glazing layer on freshness preservation of bream (Megalobrama amblycephala) during superchilling storage. *Food Control, 69*, 339–345. https://doi.org/10.1016/j.foodcont.2016.05.019

Joukar, S. (2012). Electrocardiogram alterations following one-week consumption of Crocus sativus L. (Saffron). *EXCLI Journal, 11*, 480–486. https://pubmed.ncbi.nlm.nih.gov/27418921.

Kriegel, C., Kit, K. M., McClements, D. J., & Weiss, J. (2009). Influence of surfactant type and concentration on electrospinning of chitosan–poly (ethylene oxide) blend nanofibers. *Food Biophysics, 4*(3), 213–228.

Lambrianidou, A., Koutsougianni, F., Papapostolou, I., & Dimas, K. (2021). Recent advances on the anticancer properties of saffron (crocus sativus L.) and its major constituents. *Molecules, 26*(Issue 1). https://doi.org/10.3390/molecules26010086

Li, Y., Lim, L.-T., & Kakuda, Y. (2009). Electrospun zein fibers as carriers to stabilize (−)-Epigallocatechin gallate. *Journal of Food Science, 74*(3), C233–C240. https://doi.org/10.1111/j.1750-3841.2009.01093.x

Liu, Z.-P., Zhang, Y.-Y., Yu, D.-G., Wu, D., & Li, H.-L. (2018). Fabrication of sustained-release zein nanoparticles via modified coaxial electrospraying. *Chemical Engineering Journal, 334*, 807–816. https://doi.org/10.1016/j.cej.2017.10.098

Mirhadi, E., Nassirli, H., & Malaekeh-Nikouei, B. (2020). An updated review on therapeutic effects of nanoparticle-based formulations of saffron components (safranal, crocin, and crocetin). *Journal of Pharmaceutical Investigation, 50*(1), 47–58. https://doi.org/10.1007/s40005-019-00435-1

Moradkhannejhad, L., Abdouss, M., Nikfarjam, N., Mazinani, S., & Heydari, V. (2018). Electrospinning of zein/propolis nanofibers; antimicrobial properties and morphology investigation. *Journal of Materials Science: Materials in Medicine, 29*(11), 1–10.

Najafi, Z., Kahn, C. J. F., Bildik, F., Arab-Tehrany, E., & Şahin-Yeşilçubuk, N. (2021). Pullulan films loading saffron extract encapsulated in nanoliposomes; preparation andcharacterization. *International Journal of Biological Macromolecules*. https://doi.org/10.1016/j.ijbiomac.2021.07.175

Najafi, Z., Zahran, H. A., Şahin-Yeşilçubuk, N., & Gürbüz, H. (2022). Effect of different extraction methods on saffron antioxidant activity, total phenolic and crocin contents and the protective effect of saffron extract on the oxidative stability of common vegetable oils. *Grasas y Aceites, 73*(4), e480. on press.

Okmen, G., Kardas, S., Bayrak, D., Arslan, A., & Cakar, H. (2016). The antibacterial activities of Crocus sativus against mastitis pathogens and its antioxidant activities. *World Journal of Pharmacy and Pharmaceutical Sciences, 5*(3), 146–156.

Okutan, N., Terzi, P., & Altay, F. (2014). Affecting parameters on electrospinning process and characterization of electrospun gelatin nanofibers. *Food Hydrocolloids, 39*, 19–26. https://doi.org/10.1016/j.foodhyd.2013.12.022

Özogul, Y., Durmus, M., Ucar, Y., Özogul, F., & Regenstein, J. M. (2016). Comparative study of nanoemulsions based on commercial oils (sunflower, canola, corn, olive, soybean, and hazelnut oils): Effect on microbial, sensory, and chemical qualities of refrigerated farmed sea bass. *Innovative Food Science & Emerging Technologies, 33*, 422–430. https://doi.org/10.1016/j.ifset.2015.12.018

Parray, J. A., Kamili, A. N., Hamid, R., Reshi, Z. A., & Qadri, R. A. (2015). Antibacterial and antioxidant activity of methanol extracts of Crocus sativus L. c.v. Kashmirianus. *Frontiers in Life Science, 8*(1), 40–46. https://doi.org/10.1080/21553769.2014.951774

Popović-Djordjević, J. B., Kostić, A.Ž., & Kiralan, M. (2021). In C. M. B. T.-S. Galanakis (Ed.), *41–97Chapter 2 - antioxidant activities of bioactive compounds and various extracts obtained from saffron*. Academic Press. https://doi.org/10.1016/B978-0-12-821219-6.00002-6.

Ramakrishna, S., Fujihara, K., Teo, W. E., Lim, T. C., & Ma, Z. (2005). An introduction to electrospinning and nanofibers. In *An introduction to electrospinning and nanofibers*. World Scientific Publishing Co. https://doi.org/10.1142/5894.

Sarfarazi, M., Jafari, S. M., Rajabzadeh, G., & Feizi, J. (2019). Development of an environmentally-friendly solvent-free extraction of saffron bioactives using subcritical water. *LWT, 114*, Article 108428. https://doi.org/10.1016/j.lwt.2019.108428

Saroglu, O., Bekiroglu, H., & Karadag, A. (2021). In C. M. B. T.-S. Galanakis (Ed.), *183–220Chapter 5 - encapsulation of saffron bioactive compounds*. Academic Press. https://doi.org/10.1016/B978-0-12-821219-6.00005-1.

Tarantilis, P. A., Beljebbar, A., Manfait, M., & Polissiou, M. (1998). FT-IR, FT-Raman spectroscopic study of carotenoids from saffron (Crocus sativus L.) and some derivatives. *Spectrochimica Acta Part A: Molecular and Biomolecular Spectroscopy, 54*(4), 651–657. https://doi.org/10.1016/S1386-1425(98)00024-9

Thiansilakul, Y., Benjakul, S., & Richards, M. P. (2010). Changes in heme proteins and lipids associated with off-odour of seabass (Lates calcarifer) and red tilapia (Oreochromis mossambicus×O. niloticus) during iced storage. *Food Chemistry, 121* (4), 1109–1119. https://doi.org/10.1016/j.foodchem.2010.01.058

Wang, H., Hao, L., Wang, P., Chen, M., Jiang, S., & Jiang, S. (2017). Release kinetics and antibacterial activity of curcumin loaded zein fibers. *Food Hydrocolloids, 63*, 437–446. https://doi.org/10.1016/j.foodhyd.2016.09.028

Zhang, A., Shen, Y., Cen, M., Hong, X., Shao, Q., Chen, Y., & Zheng, B. (2019). Polysaccharide and crocin contents, and antioxidant activity of saffron from different origins. *Industrial Crops and Products, 133*, 111–117. https://doi.org/10.1016/j.indcrop.2019.03.009

Zheng, Q., Wang, H., Yue, L., Yan, W., Guo, H., Chen, Z., Qi, W., & Kong, Q. (2022). Effect of irradiation on volatile compound profiles and lipid oxidation in chicken powder seasoning. *Radiation Physics and Chemistry, 191*, Article 109851. https://doi.org/10.1016/j.radphyschem.2021.109851

Zhou, Q., Li, P., Fang, S., Liu, W., Mei, J., & Xie, J. (2019). Preservative effects of gelatin active coating enriched with eugenol emulsion on Chinese seabass (lateolabrax maculatus) during superchilling (−0.9 °C) storage. *Coatings, 9*(Issue 8). https://doi.org/10.3390/coatings9080489

Zhu, G., Zhao, L. Y., Zhu, L. T., Deng, X. Y., & Chen, W. L. (2017). Effect of experimental parameters on nanofiber diameter from electrospinning with wire electrodes. *IOP Conference Series: Materials Science and Engineering, 230*, Article 12043. https://doi.org/10.1088/1757-899x/230/1/012043